

A Combined *Ab Initio* Quantum Mechanical and Molecular Mechanical Method for Carrying out Simulations on Complex Molecular Systems: Applications to the $\text{CH}_3\text{Cl} + \text{Cl}^-$ Exchange Reaction and Gas Phase Protonation of Polyethers

U. Chandra Singh and Peter A. Kollman

Department of Pharmaceutical Chemistry, School of Pharmacy, University of California, San Francisco, California 94143

Received 20 August 1985; accepted 14 March 1986

We present an approach to couple *ab initio* quantum mechanical geometry optimizations with molecular mechanical optimizations, with the added capability to carry out molecular dynamics simulations of the systems to search for new local minima. The approach is applied to the aqueous solution $\text{CH}_3\text{Cl} + \text{Cl}^-$ exchange reaction and the gas phase protonation of polyethers.

INTRODUCTION

The computer simulation of complex aperiodic chemical systems cannot be effectively accomplished using only quantum mechanical methods, since they are quite time consuming to employ. Nonetheless, they are required for systems where chemical bonds are being formed/broken or the electronically excited states of the system are of interest.

The way out of the above dilemma is to use quantum mechanical methods to treat the part of the system where chemical change or electronic excitation is taken place, while using molecular mechanical methods to describe the rest of the system. This is the philosophy behind the consistent force-field method employed by Warshel and Karplus¹ and Birge² to study electronic properties of models of visual pigments. Warshel and Levitt³ combined a MINDO/2 quantum mechanical approach with a molecular mechanical approach to simulate the strain energy of the Michaelis complex and ionic intermediate in the carbohydrate hydrolysis catalyzed by lysozyme. More recently, Warshel⁴ has shown that an empirical valence bond approach can be effectively combined with molecular mechanics to simulate complex systems.

Allinger and co-workers have used quantum mechanical methods in their MMPI⁵ approaches to determine the bond lengths of conjugated systems, in order to use these bond lengths as equilibrium values in a molecular mechanics optimizations. Houk and co-workers⁶ have used *ab initio* quantum mechanical methods to determine transition state geometries for the reacting parts of a system. After creating appropriate molecular mechanical parameters for those reacting parts, they have combined them with standard parameters for the parts of the system where no bond formation occurs, in order to estimate strain in the transition state and relative chemical reactivity.

Bolis *et al.*⁷ used a combination of *ab initio* quantum mechanics and molecular mechanics to assess the charge state of the His-Cys catalytic diad in papain. Alagona *et al.*⁸ studied the proton transfer reaction in triose phosphate isomerase and showed how the combination of *ab initio* quantum mechanics and molecular mechanics enabled the study of a chemical reaction in the presence and absence of the enzyme. This study led to insights on how the enzyme was so efficient, in that the rate limiting step is product dissociation, as well as giving a new idea on why

a genetically engineered mutant enzyme (His 95 → Gln 95) might lead to a less effective enzyme. Weiner *et al.* studied amide hydrolysis in the gas phase, in aqueous solution⁹ and in the enzyme active site of trypsin.¹⁰ They were able to simulate the energetics of amide hydrolysis in solution with surprising accuracy and to show how trypsin significantly facilitated this hydrolysis compared with the uncatalyzed reaction. Finally, Chandrasekhar *et al.*¹¹ used a combination of *ab initio* quantum mechanical calculations and umbrella sampling Monte Carlo to accurately describe the potential for the reaction $\text{Cl}^- + \text{CH}_3\text{Cl} \rightarrow \text{CH}_3\text{Cl} + \text{Cl}^-$ in the gas phase and in solution.

The above examples show the power of combining molecular mechanics with accurate quantum mechanical calculations. Nonetheless, the main problem with this approach is its computer intensive nature, in that a single energy evaluation using *ab initio* quantum mechanical calculations is a number of orders of magnitude more time consuming than the corresponding operation using molecular mechanics.

Another problem with the studies above that combine *ab initio* quantum mechanics with molecular mechanical is that they have not coupled the geometry optimization of both the molecular mechanical and quantum mechanical parts of the system, as was done with the semiempirical quantum mechanical/molecular mechanical approaches.^{3,4} The study presented here is an attempt to effectively couple the *ab initio* quantum mechanical calculations with molecular mechanical and molecular dynamical in one system of programs, in which the analytical gradients calculated in both methods are combined in an effective way to geometry optimize the structure of the system and to evaluate its combined quantum mechanical and molecular mechanical energy. The approach is then applied to two systems of recent interest. First, the Cl⁻ exchange reaction simulated so accurately by Chandrasekhar *et al.*,¹¹ has been studied, representing the CH₃Cl and Cl⁻ quantum mechanically and the H₂O molecular mechanically. Even though our calculations do not have the quantitative accuracy found in the earlier study, the large effect of the solvent in raising the barrier of the reaction is clear from our study as well, and the

time required for the calculation is relatively small. Secondly, the proton affinity of cyclic and noncyclic alkyl ethers has been calculated and increases of up to 50 kcal/mole over the proton affinity of dimethyl ether has been found for these molecules, in reasonable qualitative agreement with experiment.¹² These calculations treat the dimethyl ether part of the molecule as quantum mechanical and the rest of the ether as molecular mechanical.

METHODS

We have modified the quantum chemistry program Gaussian 80 UCSF¹³ and AMBER¹⁴ to create a link between the two. We have called this program, which has as its grandfather Gaussian 80, QUEST (Quantum Energies for Simulations and Trajectories).¹⁵ We describe this interface (QUEST for AMBER), using the example of protonation of 18-crown-6 to illustrate the method of combined quantum mechanical (dynamical) simulations. We note that our interface in Gaussian 80 is reasonably general, and it could with not too much effort equally well be coupled to other molecular mechanics/dynamics programs. We intend to submit it to QCPE.

The calculation is begun by constructing a topology file for the molecule using AMBER. This molecule is then energy refined using molecular mechanics. For the parts of the molecule that will be subsequently energy optimized using quantum mechanics, for which one may have no molecular mechanical parameters available, one would, of course, use as reasonable approximations for the equilibrium bond lengths, angles, and dihedral angles as one could. For example, in the crown ether example, for the protonated dimethyl ether "quantum mechanical fragment" separated by the dotted lines (Fig. 1), one could use $\theta_0 = 109.5^\circ$ for all internal angles, $R_0(\text{C}-\text{H}) = 1.09 \text{ \AA}$, $R_0(\text{C}-\text{C}) = 1.54 \text{ \AA}$, $R(\text{C}-\text{O}) = 1.43 \text{ \AA}$, $V_3/2 (\text{X}-\text{C}-\text{O}-\text{X}) = 2 \text{ kcal/mole}$ (by analogy with dimethyl amine), $V_3/2 (\text{X}-\text{C}-\text{C}-\text{X}) = 2.8 \text{ kcal/mole}$ (typical C-C dihedral) and $V_2/2 (\text{O}-\text{C}-\text{C}-\text{O}) = 0.5 \text{ kcal/mole}$ (stereoelectronic effect). The van der Waals parameters have come from standard molecular mechanics types and one could either estimate the appropriate partial electrostatic

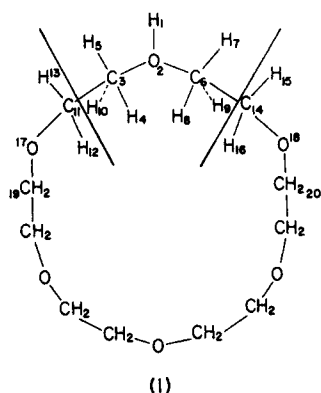


Figure 1. Schematic representation of division of protonated 18—crown—6 into quantum mechanical atoms (Q set), molecular mechanical atoms (M set) and junction atoms.

charge for this fragment from analogous fragments or carry out a single-point quantum mechanical calculation on a model for the fragment.¹⁶ For this initial optimization even zeroing the partial charges would be adequate in many cases, since the calculated molecular mechanics *geometries* are rather insensitive to the partial charges used.¹⁷

The user of the program then specifies which atoms are "quantum mechanical", [atoms 1–8, (1) Q set] which are "molecular mechanical" (M set, the remaining atoms) and which are "junction dummy atoms" [atoms 9, 10 (1)].

One then begins the quantum mechanical optimization on atoms 1–10, with the remaining atoms held rigid in Cartesian space. After one calculates the quantum mechanical gradients, one adds to these the molecular mechanical gradients on the quantum mechanical atoms, e.g., C₃ has a contribution to its gradient from the C₃—C₁₁ bond, the H₁₃—C₁₁—C₃, H₁₂—C—C₃, O₁₇—C₁₁—C₃ angles and the C₁₉—O₁₇—C₁₁—C₃ dihedral angle, as well as the nonbonded interactions (van der Waals and electrostatic) from the remaining molecular mechanical atoms. These combined gradients are used to optimize the geometry of the quantum mechanical atoms until the r.m.s. gradient on these atoms is less than some specified threshold. At this point, the molecular mechanical atoms can be energy optimized while keeping the quantum mechanical atoms fixed. In addition, one can carry out molecular dynamical calculations and then "anneal" the molecular mechanical atoms¹⁸ and do this repeatedly to search for

other local energy minima in the molecular mechanical surface.

How are the junction dummy atoms treated? They are part of the quantum mechanical calculation and "feel" gradients only from the remaining quantum mechanical atoms. However, their presence leads to gradients on, e.g., C₃ from both C₁₁ (a molecular mechanical bond energy) and H₁₀ (from the quantum mechanical gradients). In principle, one could attempt to correct for this duplication by appropriately scaling such gradients empirically, but, such corrections are likely to lead to rather small effects on the calculated energies and geometries.

There is an alternative way of handling the electrostatic nonbonded interactions of the molecular mechanical atoms with the quantum mechanical atoms. One can include the partial charges in the one electron Hamiltonian during the quantum mechanical energy and gradient calculations. In this way, both the electrostatic interaction and the polarization of the quantum mechanical atoms by the molecular mechanical can be calculated; the method described above in which molecular mechanical partial charge-quantum mechanical partial charge (electrostatic) interactions are included in the energy and gradient strictly classically do not include the polarization effect. Of course, when one includes the molecular mechanical partial charges in the one electron Hamiltonian, one only includes electrostatic interactions involving atoms at least three bonds removed from any quantum mechanical atom.

Elsewhere, we have shown, at least in the interaction of formamide-OH[−] with H₂O molecules,⁹ that the polarization effect is expected to be small in comparison with the electrostatic energy, even though this effect may well have a nonnegligible magnitude. A reasonable compromise is to only evaluate this polarization effect after the system has been energy optimized with only electrostatic interactions, since the calculated geometries are expected to be even less sensitive to the inclusion of the polarization energies than to the inclusion of the electrostatic effects. Of course, the polarization of the molecular mechanical atoms by the quantum mechanical atoms is evaluated by classical formulas after the geometry of both sets of atoms have been energy optimized.

Once geometry optimization has been completed, we need to evaluate the energy of the system. The total energy, E_T , (without polarization included) is

$$E_T = E_{QM} + E_{MM} + E_{QM/MM} \quad (1)$$

and with polarization of the molecular mechanical atoms by the quantum mechanical is

$$E'_T = E_{QM} + E_{MM} + E_{QM/MM} + E_{Pol}(QM/MM) \quad (2)$$

and with polarization of the molecular mechanical atoms by the quantum mechanical and quantum mechanical by the molecular mechanical is

$$E''_T = E'_{QM} + E_{MM} + E'_{QM/MM} + E_{Pol}(QM/MM) \quad (3)$$

where E_{QM} is the quantum mechanical energy of atoms 1–10 (protonated dimethyl ether, Fig. 1),

$$E_{MM} = \sum_{\text{bonds}} K_b(R - R_0)^2 + \sum_{\text{angles}} K_a(\theta - \theta_0)^2 + \sum_{\text{dihedrals}} \frac{K_d}{2}[1 + \cos(n\Phi - \gamma)] + \sum_{\text{nonbonded}} \left[\frac{B_{ij}}{R_{ij}^{12}} - \frac{A_{ij}}{R_{ij}^6} + \frac{q_i q_j}{\epsilon_{ij} R_{ij}} \right] + \sum_{\text{H bonds}} \left[\frac{C_{ij}}{R_{ij}^{12}} - \frac{D_{ij}}{R_{ij}^{10}} \right] \quad (4)$$

which is the standard molecular mechanical expression for the energy. E_{MM} only contains interactions involving *exclusively* atoms in the M set (Fig. 1).

$$E_{QM/MM} = \sum_{\text{bonds}} K_b(R - R_0)^2 + \sum_{\text{angles}} K_a(\theta - \theta_0)^2 + \sum_{\text{dihedrals}} \frac{K_d}{2}[1 + \cos(n\Phi - \gamma)] + \sum_{\text{nonbonded}} \left[\frac{B_{ij}}{R_{ij}^{12}} - \frac{A_{ij}}{R_{ij}^6} + \frac{q_i q_j}{\epsilon_{ij} R_{ij}} \right] + \sum_{\text{H bonds}} \left[\frac{C_{ij}}{R_{ij}^{12}} - \frac{D_{ij}}{R_{ij}^{10}} \right] \quad (5)$$

where the bond, angle, and dihedral energies involve only terms with at least one atom in both the Q and M sets and in the nonbonded term, the sum over i involves only atoms in the M set and the sum over j involves only atoms in the Q set.

After carrying out an SCF calculation to determine the dipoles induced on the atoms of

the M set by the Q set,

$$E_{POL} = -\frac{1}{2} \sum_i^M \alpha_i \vec{E}_i \cdot \vec{E}_i \quad (6)$$

where \vec{E}_i is the electric field on atom i due to all charges of the Q set and α_i is the polarizability of i th atom.

If, on the other hand, the partial charges of the M atoms are included in the one electron Hamiltonian of the quantum mechanical calculation, the quantum mechanical energy is now E'_{QM} , which includes the polarization of the quantum mechanical atoms by the molecular mechanical. In this case, to evaluate the total energy [eq. (3)], one must use a modified $E_{QM/MM}$, $E'_{QM/MM}$, where the nonbonded sum [eq. (5)] does not include any electrostatic interactions, these having incorporated in E'_{QM} .

RESULTS

In Table I we report the various energy components for the simulation of the CH₃Cl + Cl⁻ exchange reaction. This is a simple application of our approach where the Q set is the solute CH₃Cl₂⁻ and the M set are all the waters. We began that study by placing a Cl⁻ 6.014 Å from the CH₃Cl carbon along the C₃ axis pointing toward the hydrogens and carrying out a 6-31G* *ab initio* optimization of the remaining degrees of freedom. We then solvated that system by placing it at the center of mass of a 50 Å cube from a Monte-Carlo simulation of water molecules and keeping all the water molecules that were within 15 Å of any solute atom for a total of 220 water molecules.⁹ The empirical parameters used in the molecular mechanics/dynamics part of the simulation are given in ref. 19. Molecular mechanical optimization to an r.m.s. gradient of 0.1 kcal/mol Å was followed by 2 picoseconds of molecular dynamics and a further molecular mechanical optimization to a gradient of 0.01 kcal/mol Å. These molecular mechanical/dynamical simulations were carried out allowing the waters to move while keeping the solute fixed. A second quantum mechanical optimization with $R(\text{Cl}-\text{C}) = 4.571$ Å was carried out, followed by placing the solute in the same water "bath" and carrying out the same steps of molecular mechanical/dynamical op-

Table I. Energetics of CH_3Cl^- exchange reaction.

$R(\text{C} \dots \text{Cl}) (\text{\AA})^a$	E_{QM}^b	$E_{\text{QM/MM}}^c$	$E_{\text{QM/MM}} + E_{\text{MM}}^d$	E_T^e	$E_T'^f$	$E_T''^g$
6.014	0	-131.1	-1208.2	0	0(0)	0
4.571	-2.6	-126.5	-1211.0	-5.4	-0.2(-0.3)	-9.8
3.274	-6.7	-109.3	-1201.0	0.5	0.2(5.5)	-3.7
2.682	-1.0	-101.5	-1196.9	10.3	10.5(6.2)	6.6
2.383	7.2	-92.3	-1197.1	18.3	22.8(27.2)	18.6

^a $\text{C} \dots \text{Cl}$ distance along reaction pathway in \AA ; $R = 2.383 \text{ \AA}$ corresponds to pentagonal bipyramid with both $\text{C} \dots \text{Cl}$ distances equal.

^bRelative quantum mechanical energy of isolated CH_3Cl^- system relative to $E(R = 6.014 \text{ \AA}) = -958.6249 \text{ a.u.}$

^cNonbonded interactions of the quantum mechanical system (CH_3Cl_2^-) with the water molecules in kcal/mole. $E(R = 6.014 \text{ \AA}) = -958.83390 \text{ a.u.}$

^dMolecular mechanical interaction energy (water-solute relative to 6.014 \AA structure (water-solute + water-water)).

^e $E_T = E_{\text{QM}} + E_{\text{MM}} + E_{\text{QM/MM}}$, relative to $R = 6.014 \text{ \AA}$ structure.

^fRelative to $E_{\text{QM}} + E_{\text{QM/MM}} + E_{\text{MM}}$ with E_{MM} evaluated using the relative water-water energies of the nine (in parentheses, twelve) waters closest to the Cl atoms.

^gRelative $E_{\text{QM}} + E_{\text{MM}} + E_{\text{Pol}}$ (QM/MM) in kcal/mole.

timization. The same procedure was carried out for the other three geometries.

The results of the quantum mechanical calculations were, as expected, identical to those reported by Chandresekhar *et al.*¹¹ The molecular mechanical/dynamical simulations lead to optimized water structures around the ions and we used the AMBER analysis programs to calculate the solute-water energies ($E_{\text{QM/MM}}$) and water-water energies (E_{MM}). The sum of these terms as well as $E_{\text{QM/MM}}$ itself are reported in Table I and illustrate the fact that, as the Cl^- attacks the CH_3Cl and the negative charge is delocalized, the solute-water interaction energies become less favorable. If one just considered the solute-solvent ($E_{\text{QM/MM}}$) energies and E_{QM} , one calculates a barrier to Cl^- exchange, starting with the $R = 6.014 \text{ \AA}$ structure, of 46 kcal/mol. However, the inclusion of water-water energies ($E_{\text{QM/MM}} + E_{\text{MM}}$) leads to a total energy (E_T) in which the barrier comes out 23.7 kcal/mole, with the ion-dipole complex at 4.571 \AA a minimum. This minimum is not found in the full Monte-Carlo simulations carried out by Chandresekhar *et al.*¹¹ It is probably an artifact in our calculations caused by edge effects in the water cage, since we did not use periodic boundary conditions in the simulation. The $R = 6.014 \text{ \AA}$ structure would indeed be the one we expect to be most affected by edge effects, since it has the most highly charged anion and is the one closest to the "edge" of the waters. To get around this, we have earlier⁹ suggested using only the waters in the first coordination sphere of the solute to

compare the water-water energies. Although there is no clear minimum in the radial distribution of $\text{O} \dots \text{Cl}$ in our calculations, there are small breaks at 9 and 12 H_2O molecules. Thus, we have calculated the relative solvent-solvent energy for the 9 (or 12) waters nearest the Cl atoms in the five structures, and have added this to $E_{\text{QM}} + E_{\text{QM/MM}}$ to determine E_T' . Although the intermediate energies differ in magnitude, there is no ion-dipole "well" with this approach and the calculated ΔE^\ddagger for the reaction is 23–27 kcal/mol for these two models, both in respectable agreement with full simulations and experiments (see ref. 11) which suggest a ΔE^\ddagger of 23 kcal/mol and no ion-dipole "well".

The calculated polarization energies for these five structures are nearly identical, differing by only 4 kcal/mol out of a total of $\sim -640 \text{ kcal/mol}$ for the five structures. The 6.01 \AA and transition state structures are less stabilized by $\sim 4 \text{ kcal/mol}$ than the other three structures, which leads to a deepening in the ion-dipole minimum found in E_T , but the overall barrier for the reaction is $\sim 28 \text{ kcal/mol}$, still in respectable agreement with full simulations and experiments. Again, it is likely that "edge effects" contribute to the smaller polarization energy of the 6.01 \AA structure. In summary, the various models presented here as well as our previous study all can reproduce the solution ΔH^\ddagger in the Cl^- exchange reaction within the accuracy of the full Monte-Carlo simulation,¹¹ but such models are not accurate enough to assess the more subtle details of the potential sur-

face, i.e., the presence or absence of an ion-dipole "well" in solution.

In the second set of applications, we have studied the role of environment on the proton affinity of ethers in the gas phase by using the combined quantum/molecular mechanical approach. These studies were stimulated by the experimental work of Sharma *et al.*¹² and Mautner,²⁰ who carried out gas phase experiments on protonation of various polyethers. The empirical parameters used are described in ref. 21. The focus of our study is the proton affinity of open chain polyethers, i.e., glymes G1—G4 (CH₃—O(CH₂—CH₂—O)_nCH₃≡Gn) and closed chain polyethers, (O—CH₂—CH₂)_n≡Crn with dioxane≡Cr2) and how these differ from the proton affinity of dimethylether CH₃-O-CH₃. As described in methods, we carried out molecular mechanics calculations on the unprotonated form and the protonated form of each of these molecules. This was followed by a subsequent quantum mechanical/molecular mechanical optimization of the protonated forms of these molecules. Our calculations to evaluate the proton affinities of the various polyethers used the following equations

$$\Delta E = E_{QM}^{prot} + E_{QM/MM}^{prot} + E_{MM}^{prot} + E_{Pol}^{prot} \\ - (E_{QM}^{unprot} + E_{QM/MM}^{unprot} + E_{MM}^{unprot} + E_{Pol}^{unprot}) \\ - \{E_{QM}[(CH_3)_2OH^+] - E_{QM}(CH_3OCH_3)\} \quad (7)$$

where the first four terms come from eq. (2) for the protonated species, the second four from eq. (2) for the unprotonated and the last two are the 631G* calculated quantum mechanical energies for neutral and protonated dimethyl ether itself. Given our finding that E_{QM}^{prot} is nearly identical (within ~0.2-0.5 kcal/mol) to $E_{QM}(E_{QM}[(CH_3)_2OH^+]) = -154.32750$ a.u.) we did not carry out extensive quantum mechanical optimizations on E_{QM}^{unprot} but assumed it to be $= E_{QM}(CH_3OCH_3)$. Also we found that the molecular mechanical polarization energy of the unprotonated ethers was negligible, so this was not explicitly evaluated in each case. This led to eq. (8)

$$\Delta E = E_{QM}^{prot} + E_{QM/MM}^{prot} + E_{MM}^{prot} \\ + E_{Pol}^{prot} - (E_{QM/MM}^{unprot} + E_{MM}^{unprot}) \\ - E_{QM}[(CH_3)_2OH^+] \quad (8)$$

The various contributions to ΔE are reported in Tables II and III for the glymes and crowns, along with an estimate of the entropies of the

Table II. Energy and entropy of glymes.

Molecule ^a	S_{trv}^b	Unprotonated		Molecule	S_{trv}^b	E_{trv}^c	Protonated		
		E_{trv}^c	$E_{QM/MM} + E_{MM}^d$				$E_{QM/MM} + E_{QM}^d$	E_{MM}^e	E_{Pol}^e
G1	86.5	87.9	1.8	G1H ⁺	86.4	96.4	−154.34489	3.9	−4.6
G2	108.3	126.4	3.2	G2/H ⁺ (O ₂ prot) ^f	106.7	135.1	−154.36274	8.2	−7.2
				G2/H ⁺ (O ₁ prot) ^g	103.5	135.4	−154.36274	9.4	−9.4
G3	130.2	165.1	4.6	G3/H ⁺ (O ₂ prot)	125.4	173.8	−154.37424	12.6	−7.7
G4	150.8	203.6	6.3	G4/H ⁺ (O ₂ prot) ^{h,i}	139.1	213.0	−154.39773	16.2	−11.1
				G4/H ⁺ (O ₃ prot, A) ^j	141.3	212.6	−154.38262	13.9	−12.8
				G4/H ⁺ (O ₃ prot, B) ^j	141.8	212.8	−154.38512	16.9	−11.3
DIOX (boat) ^k	75.3	75.0	22.3	DIOX/H ⁺ (boat)	74.1	83.4	−154.29389	3.1	−2.5
DIOX boat ^k	73.1	75.3	15.0	DIOX/H ⁺ (chair)	77.1	83.7	−154.32648	3.0	−2.3

^aSee text for notation.

^bTransition rotational and vibrational entropy in entropy units calculated within the rigid rotor, harmonic oscillator approximation.

^cThe transitional, rotational, and vibrational internal energy calculated within the rigid rotor, harmonic oscillator approximation(kcal/mole).

^dEnergy in atomic units, see eq. (8).

^eEnergies in kcal/mole, see eq. (8).

^fOptimized protonated G2 with proton on the inner oxygen (Fig. 2).

^gOptimized protonated G2 with proton on an outer oxygen (Fig. 2).

^hThe two low-energy optimized conformations (A and B) of G3, proton on inner oxygen.

ⁱOptimized protonated G4, proton on second oxygen from end (Fig. 2).

^jThe two low-energy conformations of G4 with proton on central oxygen.

^kBoat and chair conformations of dioxane, Cr2.

Table III. Energy and entropy of crowns.

Molecule ^a	$S_{\text{trv}}^{\text{b}}$	Unprotonated		Molecule ^a	$S_{\text{trv}}^{\text{b}}$	$E_{\text{trv}}^{\text{c}}$	Protonated		E_{MM}^{d}	$E_{\text{Pol}}^{\text{d}}$
		$E_{\text{trv}}^{\text{c}}$	$E_{\text{QM/MM}} + E_{\text{MM}}^{\text{d}}$				$E_{\text{QM/MM}} + E_{\text{QM}}^{\text{e}}$			
CR4	105.4	152.9	13.1	CR4/H ⁺	109.3	161.4	−154.37821		17.7	−11.2
CR5	128.7	191.2	12.2	CR5/H ⁺ ^f	129.9	199.7	−154.37826		16.6	−7.3
				CR5'/H ⁺ ^f	124.5	200.1	−154.38912		16.9	−13.5
CR6	149.2	229.8	15.8	CR6/H ⁺ ^f	148.4	238.5	−154.39953		26.7	−10.6
				CR6'/H ⁺ ^f	149.4	238.3	−154.37664		18.5	−6.7
				CR6''/H ⁺ ^f	142.5	238.8	−154.40259		22.7	−13.7

^aSee text for notation.^bTranslational, rotational, and vibrational entropy (in entropy units) calculated within the rigid rotor/harmonic oscillator approximation.^cTranslational, rotational, and vibrational energy (in kcal/mole) calculated within the rigid rotor/harmonic oscillator approximation.^dkcal/mole—see eq. (8).^eIn atomic units.^fVarious protonated structures of CR4, CR5, and CR6 (see Fig. 2).

various conformations. These latter terms are found by translation, rotation, and vibrational energies and constructing an approximate force field for the quantum mechanical part of the system and using the normal mode section of AMBER to calculate the entropy and internal energy.

We compare the ΔE calculated with eq. (8) with the experimental proton affinity differences relative to dimethyl ether in Table IV.

As one can see, the agreement between the calculated and experimental proton affinities are quite good for G1–G3, but only qualitative for G4, Cr4, Cr5, and Cr6. Nonetheless, the ability of the theory developed here to give sensible results is clear. The results for dioxane are an important control, since both experiments and calculations suggest essentially no enhancement in proton affinity over dimethyl ether.

There are a number of potential reasons for the observed theoretical/experimental discrepancies. First, the 631G* basis set used here somewhat overestimates molecular polarity and correction for this by scaling down the partial charges of the atoms by 20% to bring the calculated dipole moment of dimethyl ether in line with the experimental value²² of 1.3 D. Twenty percent reduction in ΔE_{calc} (Table IV) improves the agreement between calculation and experiment for the protonation of G4, Cr4, Cr5, and Cr6, but worsens the agreement for G1–G3. However, the average error is reduced from 8 kcal/mol to 4 kcal/mol for these seven molecules.

Table IV. Comparison of calculated and experimental relative proton affinity of dioxane, glymes, and crowns.^a

Molecule	ΔE_{calc}^b	ΔH_{exp}^c	ΔE_{calc}^d
Dioxane	-1	1	0
G1	14	13	11
G2	25	26	20
G3	30	32	24
G4	46	35	37
CR4	39	29	31
CR5	48	32	38
CR6	54	39	43

^aEnergies in kcal/mole.^bCalculated ΔE in kcal/mole using eq. (8) and data in Tables II and III.^cExperimental data from ref. 12.^dCalculated $\Delta E'$ (scaling down ΔE by 20%).

Table II and III contain a number of entries for G4 (O₂ or O₃ protonation, with two conformations considered for the latter), Cr5 (2 conformations), Cr6 (3 conformations). Figure 3 contains stereo views of some of these molecules and stereo views and/or xyz coordinates of the others are available on request from the authors. We cannot guarantee having found the global minimum conformation for these molecules, but since we generally *overestimate* the proton affinities, missing lower energy conformations would only worsen the theory/experiment agreement and not explain the quantitative discrepancies.

In the course of calculating entropies for these various molecules, we have found that for Cr4 and Cr6, the lowest frequency normal

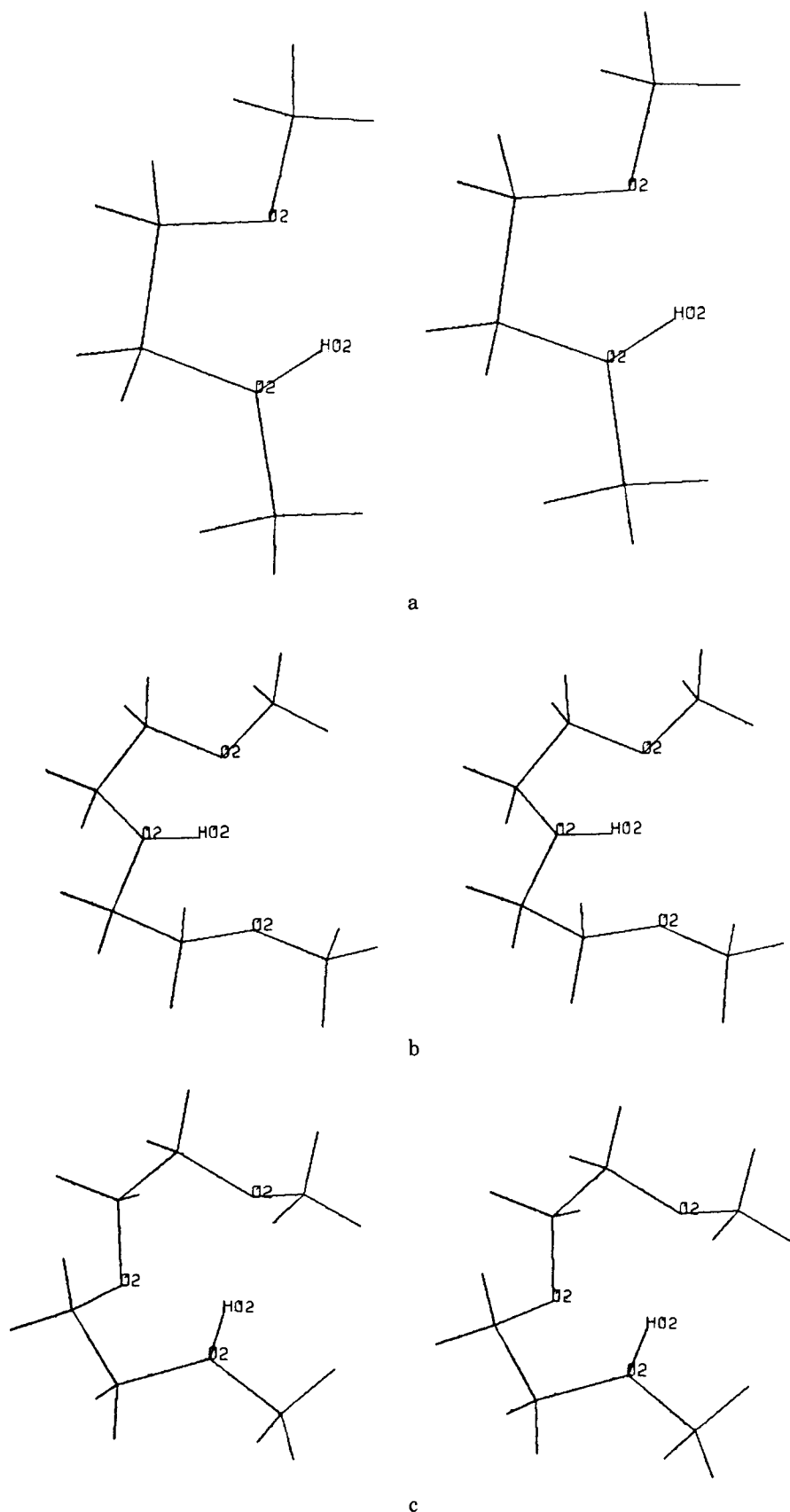
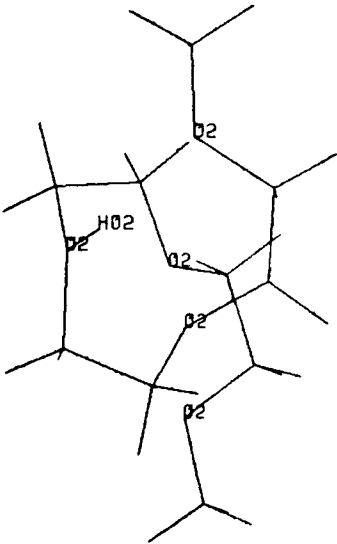
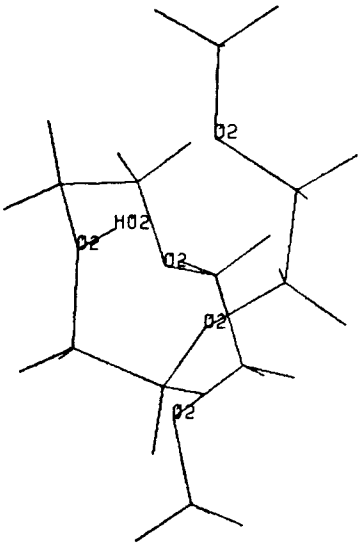
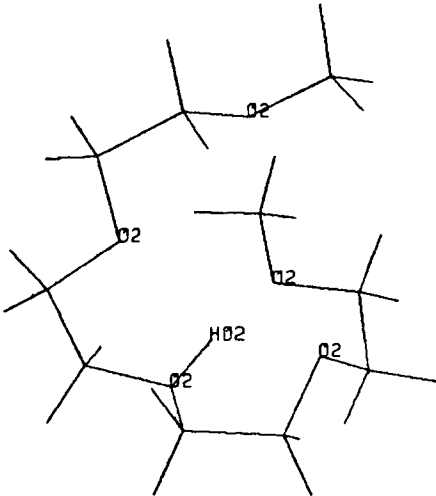
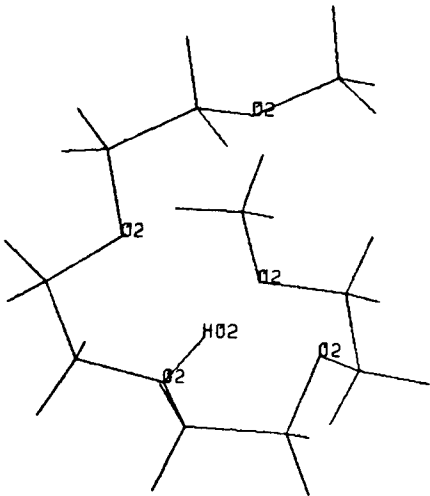


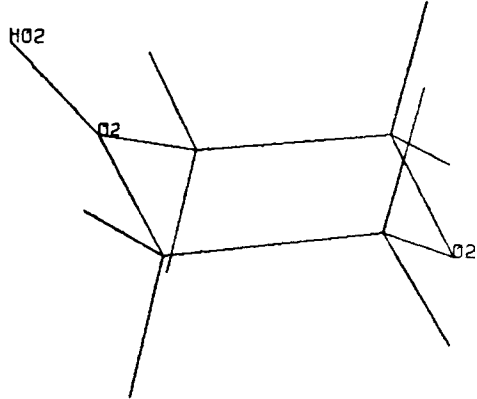
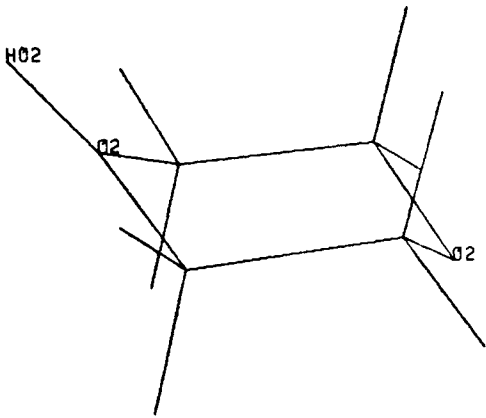
Figure 2. Stereo views of some of the structures of glymes and crowns (see Tables II and III and text for notation). (a) G1/H⁺; (b) G2/H⁺ (O₂ prot); (c) G2/H⁺ (O₁ prot); (d) G4/H⁺ (O₂ prot); (e) G4/H⁺ (O₃ prot, A); (f) dioxane/H⁺ (chair); (g) Cr4/H⁺; (h) CR5'/H⁺; and (i) CR6''/H⁺.



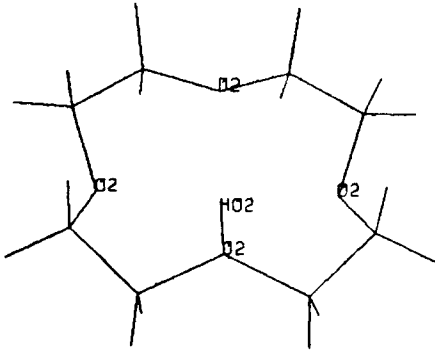
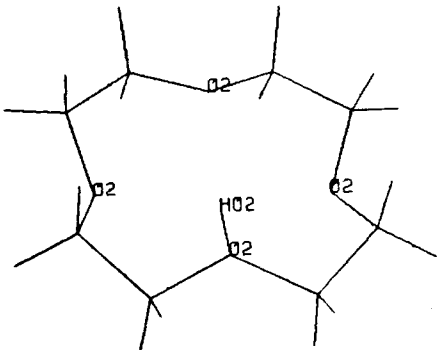
d



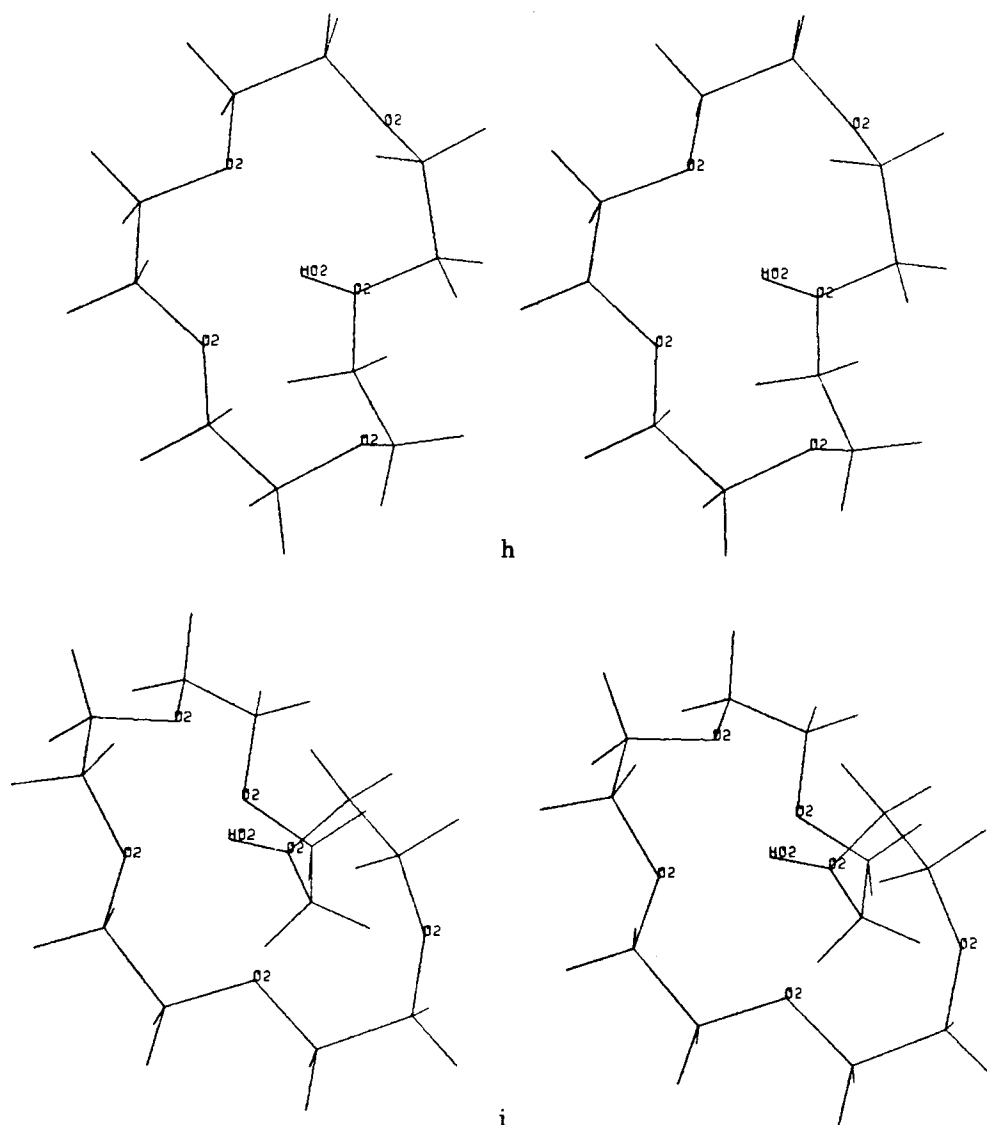
e



f



g



mode of the protonated molecule is actually *lower* (Table V) than the lowest frequency mode of the unprotonated molecule. This somewhat surprising result has precedent in our earlier studies of Li⁺/spherand complexes,²³ where the presence of a positive charge "softens" the effective O.....O repulsion in this molecule.

Our estimated ΔS (relative to dimethyl ether) of the protonation reaction are significantly smaller than those estimated by Sharma *et al.*¹² Given that these experimental values are based on estimating ΔS protonation at only two temperatures, they are subject to large errors. On the other hand, this lack of agreement also might indicate that the true local minima in these molecules has not been found in these simulations and this local minimum is much more restricted

than those found here. It is relevant that Sharma *et al.*¹⁰ found a ΔS (relative to dimethyl ether protonation) of ~ -20 eu for *both* G4 and CR6. This appears to rule out a large negative ΔS contribution to G4 protonation coming from the *reduction* of the *number* allowed low-energy conformations in G4 compared with G4/H⁺, an effect which would be expected to be absent in comparing CR6 and CR6/H⁺. This effect was also not considered here because we use an all trans model for unprotonated G2, G3, and G4.

In their experiments, Sharma *et al.*¹² also studied molecules DM4 and DM5, the latter of which is similar in structure to G2. DM5 has a ΔPA relative to dimethyl ether of 29.4 kcal/mol, similar to what is found for G2.

Sharma *et al.*¹² have interpreted their results in terms of structures found in inter-

Table V. Lowest vibrational frequencies of Glymes and Crowns (cm^{-1}).^a

G1	73, 121, 141, 181
G1/H ⁺	92, 119, 150
G2	39, 70, 85, 93, 125, 153, 176
G2/H ⁺	49, 74, 109, 120, 159, 197
G3	21, 50, 55, 57, 96, 103, 126, 140, 142, 166, 168, 194
G3/H ⁺	33, 45, 84, 89, 109, 111, 154, 171, 199
G4	18, 28, 39, 52, 64, 80, 90, 107, 120, 134, 143, 155, 176, 186
G4/H ⁺	25, 36, 74, 85, 93, 105, 109, 118, 139, 145, 189
Cr4	86, 108, 143, 154, 182, 199
Cr4/H ⁺	46, 95, 138, 147, 170, 188
Cr5	44, 63, 71, 88, 89, 120, 138, 152, 154, 193
Cr5'/H ⁺	44, 52, 85, 91, 113, 140, 154, 157, 167, 195
Cr6	37, 37, 60, 60, 69, 113, 117, 129, 129, 153, 153, 158
Cr6''/H ⁺	42, 52, 71, 77, 92, 112, 118, 137, 142, 156, 175, 196
Cr6/H ⁺	16, 35, 48, 75, 84, 100, 124, 128, 150, 163, 169, 188

^aFrequencies $<200 \text{ cm}^{-1}$ reported for lowest energy isomer of each molecule, except for Cr6/H⁺ where the two results for the two lowest energy structures are presented.

actions of $(\text{CH}_3)_2\text{O}$ with $(\text{CH}_3)_2\text{OH}^+$, $\text{O} \dots \text{H} \dots \text{O}$, where the hydrogen is equally shared between oxygens and the $\text{O} \dots \text{O}$ distances are $\sim 2.4\text{--}2.5 \text{ \AA}$. To study such structures with the approach used here would require treating at least two oxygens quantum mechanically and the remainder by molecular mechanics. The software presented here is capable of doing this, but the disk space to study the quantum mechanical optimization $(\text{CH}_3)_2\text{O} \dots \text{H}^+ \dots \text{O}(\text{CH}_3)_2$ at the 631G* quantum mechanical level is not currently available. Such structures might have significantly lower entropies than the localized oxygen protonated structures presented here, but that is not certain without further calculation. Nonetheless, the calculated *energies* of the structures presented here suggest that the presence of proton sharing oxygens is *not essential* to explain the experimental results, i.e., structure with the proton mainly on one oxygen can be sufficiently stabilized by nearly oxygen dipoles and polarizable $-\text{CH}_2-$ groups to explain much of the difference in proton affinity relative to CH_3OCH_3 .

It is clear from many quantum mechanical studies on $\text{B}_1 \cdot \text{H}^+ \text{B}_2$ that the presence of a single well potential requires an $R(\text{B}_1 \dots \text{B}_2) \sim 2.4\text{--}2.5 \text{ \AA}$ and a near linear $\text{B}_1\text{H} \dots \text{B}_2$ bond. In the noncyclic G1—G4 structures and Cr4—Cr6, such a distance can be achieved, but to also achieve a near linear directionality of the $\text{O} \dots \text{O}$ dipolar orientation may be more difficult. In fact, in G2/H⁺, such a conformation can be achieved $\{[R(\text{O}_1 \dots \text{O}_3) = 2.4 \text{ \AA}, \theta(\text{O}_1 - \text{H}_1 \dots$

$\text{O}_3) = 180^\circ R(\text{O}_1 - \text{H}) = R(\text{O}_3 - \text{H}) = 1.2 \text{ \AA}]\}$, but with a molecular mechanical strain energy that is likely to be greater than G2/H⁺ presented in Table II. We cannot unequivocally resolve this issue here, but our energy results suggest that the various polyethers G2—G4 and Cr4—Cr6 can achieve their impressive ΔPA relative to DME by dipole alignment alone, without significant contribution from proton sharing.

DISCUSSION AND CONCLUSIONS

We have presented an approach to couple *ab initio* quantum mechanical calculations with molecular mechanical, have implemented it by modifying Gaussian 80 UCSF¹³ and AMBER¹⁴ and have applied it to the $\text{CH}_3\text{Cl} + \text{Cl}^-$ reaction in solution and gas phase protonation of polyethers. As currently implemented, the approach uses successive quantum mechanical optimizations (with the rest of the system fixed) and molecular mechanical optimization (with the quantum mechanical atoms fixed) until the energy gradients of both systems are below a specified threshold. There is no conceptual difficulty with implementing this approach while allowing all (both quantum and molecular mechanical) of freedom to optimize simultaneously. However, with systems of many hundreds or thousands of degrees of freedom, simultaneous optimization would require hundreds of quantum mechanical energy + gradient evaluations, which would be quite computer time intensive.

It is important to place in perspective what has been demonstrated here. It has been clear for a long time that coupling of quantum mechanical and molecular approaches is useful and often necessary.¹⁻¹¹ Nonetheless, when one uses *ab initio* quantum mechanical methods, such a coupling has involved taking the results from the molecular mechanical calculation and carrying out single-point *ab initio* calculations,^{7,8,10} using quantum mechanically optimized geometries, which are held fixed during molecular mechanical optimization^{6,9} or fitting the quantum mechanical surface to an analytical function, to use in Monte-Carlo "molecular mechanical" simulations.¹¹ Our contribution here is to show how *ab initio* and molecular mechanical methods can be combined in a single computer program which can allow efficient geometry optimization, transition state searching or local minima scanning for complex molecular systems. We have demonstrated the geometry optimization and local minima scanning capabilities of the program here. In particular, this program is the first to combine *ab initio* quantum mechanical approaches with molecular *dynamical* so that new "classical" local minima can be found in the energy surface of complex reacting systems. We have used this molecular dynamical capability to find lower energy solvent structures in the Cl⁻ exchange reaction.

We have tested our approach on two sets of systems involving solvation effects on a chemical reaction and gas phase protonation of polyethers and have in the process compared our results with nine pieces of experimental data. In the case of the CH₃Cl + Cl⁻ exchange reaction, we have considered a number of alternative models, all of which lead to solvent-induced barriers in rather good agreement with experiment and the more elaborate and time consuming calculations of Chandresekhar *et al.*¹¹ In the gas phase protonation of polyethers, our calculations have been able to show that dioxane has a proton affinity little different than dimethyl ether, that successive glymes have a much larger proton affinity than dimethyl ether, increasing for glyme with two oxygens to glyme with five oxygens) from 13 to 35 kcal/mol (experimentally) and 14 to 46 kcal/mol calculated. The crown ethers 12—crown—4, 15—crown—5 and 18—

crown—6 have experimental proton affinities of 29–39 kcal/mol and calculated from 39–54 kcal/mol. We have suggested part of the discrepancies between calculated and experimental proton affinities can be attributed to the exaggerated electrostatic charges from the 631G* basis set *ab initio* model and have shown that scaling down the interaction energies by 20% reduces the discrepancies between calculated and experimental proton affinities to an average of 4 kcal/mol. Most importantly, with or without scaling, *almost all* of the relative energies are correctly ranked. The only two exceptions come from the fact that the stabilization is exaggerated more for the crowns than the glymes with the equivalent number of oxygens, so that CR4 is calculated to have a higher proton affinity than G3 and CR5 a higher proton affinity than G4. Both referees have suggested that the usefulness of our approach could have been more "convincingly" demonstrated on smaller "better defined" systems without being explicit about which systems they had in mind. Although a study of organic reactions of variously strained molecules such as those analyzed by Houk and co-workers⁶ seems worthwhile,²⁴ we feel that we have made enough contact with experimental reality to show that the approach is capable of giving reasonable results, given the uncertainties and inaccuracies in the energies at both the quantum and molecular mechanical level.

We are currently applying this approach to study the enzyme catalyzed reaction by trypsin, in which the quantum mechanical part of the system is large enough to require supercomputer resources. We feel the approach here, in which highly accurate *ab initio* energies can be combined with the powerful molecular mechanical/dynamical has promise in leading to new insights into the nature of enzyme action.

We are grateful to the NIH (GM-29072) for research support to PAK and to the UCSF Computer Graphics Lab (supported by RR-1081) for use of their facilities. The name QUEST was the result of a late night collaboration at the 1985 Gordon Conference of Proteins by Peter Rossky, Ron Raines, and P.A.K. and we are grateful to them and thank Carol Post for bringing ref. 15 to our attention.

References

1. A. Warshel and M. Karplus, *J. Am. Chem. Soc.*, **94**, 5612 (1972).

2. R. Birge, M. Sullivan, and B. Kohler, *J. Am. Chem. Soc.*, **98**, 358 (1976).
3. A. Warshel and M. Levitt, *J. Mol. Biol.* **103**, 227 (1976).
4. A. Warshel and R. Weiss, *J. Am. Chem. Soc.*, **102**, 6218 (1980).
5. N. L. Allinger and J. T. Sprague, *J. Am. Chem. Soc.*, **95**, 3893 (1973).
6. K. N. Houk, S. R. Moses, Y. D. Wu, N. G. Rondan, V. Jäger, R. Schoke, and F. R. Fromczek, *J. Am. Chem. Soc.*, **106**, 3880 (1984).
7. G. Bolis, M. Ragazzi, D. Salvadenri, D. Ferro, and E. Clementi, *Gazz. Chim. Ital.*, **108**, 425 (1978).
8. G. Alagona, P. Desmeules, C. Ghio, and P. Kollman, *J. Am. Chem. Soc.*, **106**, 3623 (1984).
9. S. Weiner, U. C. Singh, and P. Kollman, *J. Am. Chem. Soc.*, **107**, 2219 (1985).
10. S. Weiner, G. Seibel, and P. Kollman, *Proc. Nat. Acad. Sci.* **83**, 649 (1986).
11. J. Chandrasekhar, S. Smith, and W. Jorgensen, *J. Am. Chem. Soc.*, **107**, 154 (1985).
12. R. Sharma, A. Blades, and P. Kebarle, *J. Am. Chem. Soc.*, **106**, 510 (1984).
13. U. C. Singh and P. Kollman, *QCPE Bull.*, **2**, 17 (1982).
14. P. Weiner and P. Kollman, *J. Comp. Chem.*, **2**, 287 (1981).
15. We note that the name of our program is not unique; J. I. Garrels, J. T. Farrar, and C. B. Burwell in J. E. Celis and R. Bravo, Ed., *Two Dimensional Gel Electrophoresis of Proteins*, Academic Press, New York, 1984 pp 37–91 describe "The QUEST system for computer-analyzed two-dimensional electrophoresis of proteins."
16. U. C. Singh and P. Kollman, *J. Comp. Chem.*, **5**, 129 (1984).
17. B. M. Pettitt and M. Karplus, *J. Am. Chem. Soc.*, **107**, 1166 (1985).
18. F. Stillinger and T. Weber, *Science*, **225**, 983 (1984).
19. The parameters for the water were the TIPSP water model (W. Jorgensen, J. Chandrasekhar, J. Madura, R. Impey, and M. Klein, *J. Chem. Phys.*, **79**, 926 (1983)). For the solute, the nonbonded parameters for C and H were taken from S. J. Weiner, P. A. Kollman, D. A. Case, U. C. Singh, C. Ghio, G. Alagona, S. Profeta, and P. Weiner, *J. Am. Chem. Soc.*, **106**, 765 (1984); for Cl, $R^* = 1.9 \text{ \AA}$ and $\epsilon = 0.20 \text{ kcal/mole}$. The partial charges for the C, H, and Cl were determined by fitting the quantum mechanical electrostatic potential to a partial charge model. The partial charge for the five structures, in the order of Cl^- , C, H, and Cl are: $R = 6.014 \text{ \AA}$, $q = -1.000, -0.267, 0.165, -0.277$; $R = 4.571 \text{ \AA}$, $q = -0.998, -0.243, 0.166, -0.258$; $R = 3.274 \text{ \AA}$, $q = -0.978, -0.227, 0.175, -0.320$; $R = 2.682 \text{ \AA}$, $q = -0.962, -0.267, 0.217, -0.422$; $R = 2.383 \text{ \AA}$, $q = -0.759, -0.251, 0.256, -0.759$. In the polarization calculations the polarizability for the atoms was taken from experimental values: $\alpha(\text{Cl}^-) = 3.0$, $\alpha(\text{Cl}) = 2.25$, $\alpha(\text{O}) = 0.604$, $\alpha(\text{H}) = 0.386$, $\alpha(\text{C}) = 1.064$, all in \AA^3 . The polarizability was linearly interpolated for the various Cl atoms between the Cl^- and Cl values based on the partial charges.
20. M. Mautner, *J. Am. Chem. Soc.*, **105**, 4906 (1983).
21. The molecular mechanical parameters for the $-\text{CH}_2-\text{O}-\text{CH}-$ fragment of the crown ether were taken from S. J. Weiner, P. Kollman, D. Nguyen, and D. Case, *J. Comp. Chem.* (in press) with $q_{\text{C}} = 0.025$, $q_{\text{H}} = 0.074$, $q_{\text{O}} = -0.346$. The partial charges for the oxonium fragment $-\text{CH}_2-\overset{\text{H}}{\underset{+}{\text{O}}}-\text{CH}_2-$ were determined by the electrostatic potential fitting approach and were $q_{\text{C}} = 0.039$, $q_{\text{H}} = 0.194$, $q_{\text{O}} = -0.402$, $q_{\text{HO}} = 0.549$.
22. R. Nelson, D. Lide, and A. Maryott, *Nat. Bur. Stand (US) Circ.*, No. 10, 1967.
23. P. Kollman, G. Wipff, and U. C. Singh, *J. Am. Chem. Soc.*, **107**, 2212 (1985).
24. F. Brown and P. Kollman, calculations in progress.